A. MITRA, P. SAHOO, K. SAHA

RESEARCH

A Multi Asperity Model of Contact Between a Smooth Sphere and a Rough Flat Surface in Presence of Adhesion

Multi asperity elastic-plastic adhesive contact between a smooth sphere and a rough flat surface is considered. To incorporate the effect of adhesion, JKR (Johnson–Kendall–Roberts) contacts are assumed and the mixed asperity contact model for a sphere with rough flats, developed by Kagami et al, is used. The results are obtained in terms of plots of radial pressure distribution, contact radius versus load, and compliance versus load and they are studied for different conditions that arise from varying loading and material parameters. The results obtained exhibit a negative pressure region at the edge of contact. It is observed that larger sphere radius gives lower pressure distribution and lower compliance.

Keywords: *Sphere on flat, Elastic–plastic contact, Adhesion, Roughness*

1. INTRODUCTION

When two smooth and clean surfaces are brought together, a finite normal force is required to pull the two apart. This phenomenon of surfaces sticking together is known as adhesion and the force required to separate the surfaces is called force of adhesion or adhesive force. There has been a vast amount of experimental and analytical studies done in the field of adhesion and adhesive forces and there exist two widely known models for predicting the adhesive force, namely JKR model [1] and DMT model [2]. Tabor [3] compared the assumptions and predictions of the JKR and DMT models and pointed out the inconsistencies between the two. Muller et al [4] showed that the two models can be considered as two opposite extremes of adhesive contact according to a dimensionless number called Tabor parameter (μ). The effect of surface roughness on adhesion at the contact of rough solids has also been studied analytically in great detail by Roy Chowdhury and Ghosh [5] using Greenwood and Williamson's [6] rough surface model and JKR adhesion model. However, all these models consider contact between two rough flat surfaces, although contact between rough curved surfaces is also very common.

Contact of a sphere with a flat rough surface is significantly different from the case of contact between flat rough surfaces. In the former case, there exists a central region of continuous contacts because of greater deformation of the asperities. This region is surrounded by a fringe where only the taller asperities touch, and beyond this, as the gap between the surfaces widens, fewer and fewer asperities come into contact. Greenwood and Tripp [7] carried out the first analytical study of contact of rough curved surfaces and investigated the effect of roughness on contact of elastic spherical bodies. In this model contact between two spheres is approximated by contact between a sphere and a plate. Yip and Vernart [8] carried out an elastic analysis on deformation of rough spheres, rough cylinders, and rough annuli in contact. Nuri [9] considered the normal approach in the case of contact between two curved surfaces. Mikic and Roca [10] put forward an alternative numerical model by assuming plastic deformation of the asperities. Kagami et al [11] theoretically analyzed the contact between a smooth sphere and a rough plate for a mixed asperity contact theory. Bahrami et al [12] considered the effect of roughness on elastic contact of spherical bodies, assuming plastic deformation of the asperities.

A review of the existing literature reveals that work on adhesive contact of sphere with rough flat surface is limited [13]. Moreover, such an analysis is essential for developing fundamental understanding of interfacial phenomena on a small scale and for analyzing the experimental

Anirban Mitra, Prasanta Sahoo[1], Kashinath Saha
Department of Mechanical Engineering
Jadavpur University, Kolkata 700032, India
E-mail: psjume@gmail.com

observations on the contact behaviour of micro/nano-structures relevant in nano-tribology and nano-mechanics applications.

2. BASIC CONSIDERATIONS

In contact analysis of flat rough surfaces the load is expressed as a function of the separation of the two surfaces, which is constant. But for contact between a curved surface and a flat the separation between the two surfaces increases along the radial direction from the center of contact. So, a relation between the separation and the radial position is required to find out the desired results. Moreover, in the case of curved rough surface contact, the bulk or substrate of the bodies in contact is considered deformable as well as the asperities. This implies that the contact of rough curved bodies includes two problems: deformation of the substrate or bulk and deformation of the asperities. In general, the bulk deformation is considered elastic, but asperities can deform in different ways, for example, fully elastic, fully plastic, or partly elastic and partly plastic.

The present work considers a theoretical analysis of loading behaviour in the adhesive contact between a smooth sphere and a rough flat following mixed asperity model of Kagami et al [11] and RG model [5] of multi asperity adhesive contact. It is assumed that an asperity deforms elastically or plastically based on whether its deformation is below or above a critical value. This critical value of deformation of an individual asperity is obtained following the RG model, whereas the pressure distribution is calculated following the model of Kagami et al [11]. Figure 1 shows that a rough surface with a distribution, *f(z)*, of asperity heights is pressed under a load *P* by a smooth sphere of radius, *B*. It is assumed that the distribution of asperity heights is Gaussian in nature and given by,

$$f(z) = \left(1/(\sigma\sqrt{2\pi})\right)e^{-(z^2/2\sigma^2)}. \quad (1)$$

Here σ is the standard deviation of asperity height distribution. The number of asperities per unit area is taken as η_0. A pressure distribution *q(r)* is produced by the contact within a circular contact region of radius a. The coordinate r lies in a radially outward direction from the center of the contact spot. Under a load *P*, the compliance (α) between the sphere and the rough surface produced at a distance *r* from the center of the contact area is a function of the asperity deformation (*u(r)*), the elastic deformation (*w(r)*) of the sphere and the substrate of the rough flat and a distance $r^2/2B$ (shown in Figure 1) and is represented as [11],

$$\alpha = u(r) + w(r) + r^2/2B. \quad (2)$$

3. ADHESIVE CONTACT

Incorporation of adhesion in the mixed asperity model proposed by Kagami et al [11] is carried out by considering JKR contacts and using the principles of RG model. In case of contact between a smooth sphere and a flat in presence of surface forces, JKR model predicts that the load on an elastically deformed asperity is given by,

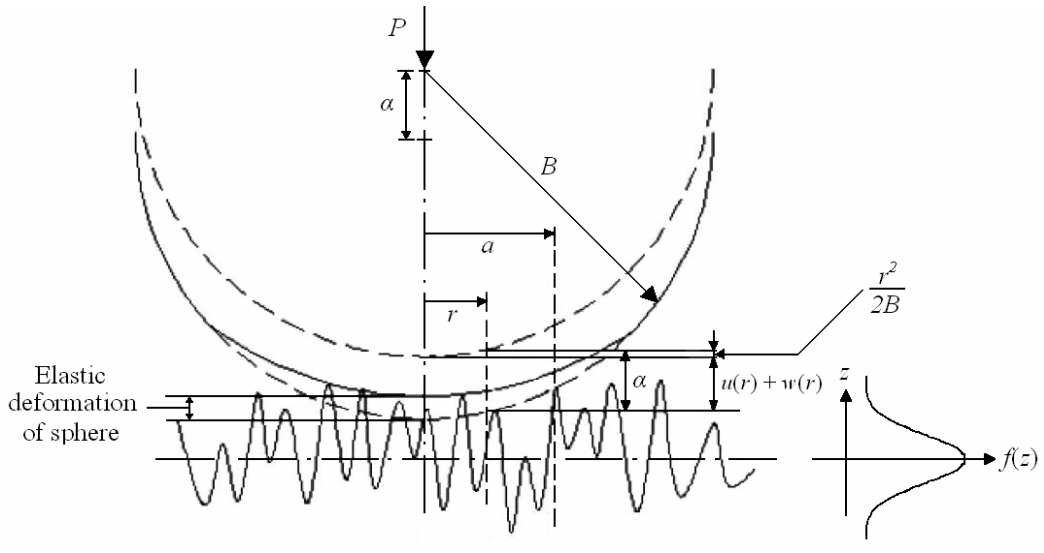

Figure 1. Contact between a smooth sphere and a rough flat surface

$$P_e = \frac{4}{3} E R^{1/2} \delta_1^{3/2} - (8\pi\gamma E)^{1/2} R^{3/4} \delta_1^{3/4} \quad (3)$$

Here E is the equivalent elastic modulus given by $E = \left[1-\nu_1^{\,2}/E_1 + 1-\nu_2^{\,2}/E_2\right]^{-1}$, γ is the work of adhesion per unit area. δ_1 is apparent displacement and R is the radius of curvature of the hemispherical asperity tip. In expression (1), the first term is the Hertzian load term and the second one is the adhesive influence term. The load on a plastically deformed asperity [14] can be obtained from an energy balance approach at the contact and is given by,

$$P_p = \pi a_p^2 H - 2\pi R\gamma \,. \quad (4)$$

Here, H is the hardness and a_p represents the contact radius during plastic loading and from geometric considerations, assuming that the change in the contact geometry owing to material flow is negligible $a_p = (2R\delta)^{1/2}$, where δ is the asperity displacement. As a modeling approximation, it is considered that plastic deformation initiates when the following condition is satisfied,

$$P_e / \pi a_e^{\,2} = H \,. \quad (5)$$

Here, a_e is the apparent Hertzian contact radius given by $(R\delta_1)^{1/2}$. Substituting equations (3) in (5) the critical displacement (δ_{c1}) to commence plastic deformation can be obtained.

$$\delta_{c1}^{3/4} - \left(\frac{\pi R^{1/2} H}{K}\right)\delta_{c1}^{1/4} - \frac{(6\pi\gamma)^{1/2} R^{1/4}}{K^{1/2}} = 0 \quad (6)$$

where, K = (4E/3). This equation provides a plasticity condition and can be solved to give the critical displacement (δ_{c1}), which distinguishes between the elastically and plastically deformed asperities. But, it must be kept in mind that δ_{c1} in the above equation is the apparent displacement corresponding to an apparent Hertzian load given by $[P_e + (6\pi\gamma K a^3)^{1/2}]$. Following Johnson, δ_1 may be expressed in terms of actual displacement: $\delta_1 = \delta + (2/3)(6\pi\gamma a/K)^{1/2}$. So, actual critical displacement δ_c can be determined from the above expression.

$$\delta_c = \delta_{c1} - 2.89(\gamma/K)^{1/2} R^{1/4} \delta_{c1}^{1/4} \quad (7)$$

The asperity deformation is determined in a similar way to the mixed asperity model proposed by Kagami et al. A pressure distribution *q(r)* is assumed depending on two constants *a* and *b* in the following form.

$$q(r) = q_0[e^{-(r/b)^2} - e^{-(a/b)^2}] \quad (8)$$

Integration of *q(r)* with respect to *r* from 0 to a gives the external load *P*. The constant term (q_0) can be found out in terms of load (*P*) and the two constants a and b as follows.

$$q_0 = \frac{P e^{(a/b)^2}}{b^2\pi\,[e^{(a/b)^2} - 1 - (a/b)^2]} \quad (9)$$

On the basis of this assumed distribution the elastic deformation (*w(r)*) of the sphere and the rough flat subsurface is found out. It is known that for a concentrated force acting on the boundary of a semi-infinite solid, the displacement in the direction of the load at the boundary plane, denoted by $z = 0$ is given by [15], $(w)_{z=0} = P\,(1-\upsilon^2)/(\pi E r)$. From this relation, displacements caused by a distributed load can be found out by superposition. In the present scenario, the case of a uniform load distributed over the area of a circle of radius *a* is considered. A point M on the surface of the body at a distance r from the center of the circle is chosen such that it lies within the loaded area i.e. $r < a$. Now, a small element of the loaded area, as shown by the shaded area in Figure 2, bounded by two radii including the angle '$d\varepsilon$' and two arcs of circle with radii 's' and 's + ds', all drawn from point 'M' is taken. The load on this element is $qs.ds.d\varepsilon$. So, after performing the necessary integrations the total deflection is $w = ((1-\upsilon^2)\,q/\pi E)\iint ds d\varepsilon$. In this derivation a uniformly distributed load is considered and so 'q' is a constant term appearing outside the double integrations. But if the load varies over the area, then the 'q' term should be kept inside the double integrations as a function the coordinates s and ε. Finally, the elastic deformation w(r) of the sphere and the substrate of the rough flat is given by,

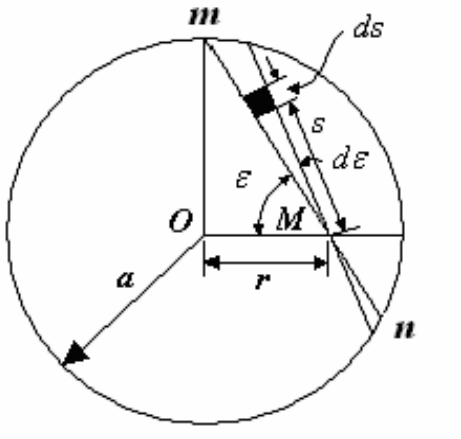

Figure 2. Circular area of radius a under distributed load showing the point M and the chosen element

$$w(r)=\frac{4q_0}{\pi E}\int_0^{\pi}\int_0^{r\cos\varepsilon+\left(a^2-r^2\sin^2\varepsilon\right)^{1/2}}[x]\,ds d\varepsilon \qquad (10)$$

with $x=e^{-(r^2+s^2-2rs\cos\varepsilon/b^2)}-e^{-(a/b)^2}$.

The asperity deformation, *u(r)*, is determined by using the following expression given by Kagami et al.

$$u(r)=(a^2-r^2)/2B+w(a)-w(r) \qquad (11)$$

Asperity deformation is a function of the radial distance (*r*) from the center of the contact. So, depending on whether at a particular radial distance (*r*), the asperity deformation (*u(r)*) is greater or less than the critical value (δ_c), the nature of the contact is determined and the corresponding pressure distribution is obtained. Expressions of the pressure distributions in non-dimensional form in terms of elastic adhesion index (θ) and plasticity index (ψ) corresponding to the different regimes of contact are given below.

Case 1: $\delta_c^* \geq u^*(0)$: Elastic contact

$$p^*(r)=\int_0^{u^*(r)}\left\{u^*(r)-z^*\right\}^{3/2}e^{-z^{*2}/2}\,dz^* - \frac{4.34}{\theta^{1/2}}\int_0^{u^*(r)}\left\{u^*(r)-z^*\right\}^{3/4}e^{-z^{*2}/2}\,dz^* \qquad (12)$$

Case 2: $\delta_c^* < u^*(0)$ and $\delta_c^* \leq u^*(r)$: Elastic-plastic contact

$$p^*(r)=\int_{u^*(r)-\delta_{c1}^*}^{u^*(r)}\left\{u^*(r)-z^*\right\}^{3/2}e^{-z^{*2}/2}\,dz^* - \frac{4.34}{\theta^{1/2}}\int_{u^*(r)-\delta_{c1}^*}^{u^*(r)}\left\{u^*(r)-z^*\right\}^{3/4}e^{-z^{*2}/2}\,dz^* + \frac{4.75}{\psi}\int_0^{u^*(r)-\delta_c^*}\left\{u^*(r)-z^*\right\}e^{-z^{*2}/2}\,dz^* - \frac{6.22}{\theta}\int_0^{u^*(r)-\delta_c^*}e^{-z^{*2}/2}\,dz^* \qquad (13)$$

Case 3: $\delta_c^* < u^*(0)$ and $\delta_c^* > u^*(r)$: Elastic contact

In this case, the normalised pressure will be given by equation (12).

In the above equations, the normalised pressure,

$$p^*(r)=\left(p(r)(2\pi)^{1/2}\right)\Big/\left(K\eta_0 R^{1/2}\sigma^{3/2}\right);$$

$$u^*(r)=u(r)/\sigma;\ z^*=z/\sigma;\ \delta_c^*=\delta_c/\sigma;$$

$$\delta_{c1}^*=\delta_{c1}/\sigma;\ \theta=K\sigma^{3/2}R^{1/2}\Big/\gamma R;$$

$\psi=(E/H)(\sigma/R)^{1/2}$; σ being the r.m.s roughness.

The calculated pressure distribution is compared with the assumed pressure distribution and until the difference between the two pressure values at r = 0 falls below a predefined error limit, the values of *a* and *b* are varied.

Equations (4) and (5) can also be written in non-dimensional form in terms of elastic adhesion index and plasticity index.

$$\delta_{c1}^{*3/4}-\frac{2.37}{\psi}\delta_{c1}^{*1/4}-\frac{4.34}{\theta^{1/2}}=0 \qquad (14)$$

$$\delta_c^*=\delta_{c1}^*-\frac{2.89}{\theta^{1/2}}.\delta_{c1}^{*1/4} \qquad (15)$$

4. RESULTS AND DISCUSSION

The equations developed in the previous sections are evaluated to obtain the non-dimensional pressure distribution along the radius of the contact spot. In addition, contact radius versus applied load and compliance versus applied load plots for variations in the sphere radius are obtained. The evaluation of the equations is carried out utilizing inbuilt MATLAB functions 'quad' and 'trapz'. The

appropriate values of a and b are determined following a trial and error method, considering the criterion of equality of assumed and calculated pressures at r = 0. For a given load, depending on the material properties, nature of adhesion, surface roughness, and radius of the sphere, the contact radius a attains a certain fixed value, and in order to find that value, the trial and error method is employed. By choosing a and b, the assumed pressure distribution is known through equations (8) and (9), and from this distribution, the elastic bulk deformation and asperity deformation are calculated with the help of equations (10) and (11), respectively. The value of u(r) thus obtained is used according to the condition satisfied (cases 1, 2, and 3 given by equations (12) and (13)) to calculate a new pressure distribution. If the termination criterion is not satisfied, a new set of *a* and *b* values is chosen, and the same process is followed until the two distributions are sufficiently close.

To compute the pressure distribution, material and surface parameters such as equivalent elastic modulus (E), hardness (H), work of adhesion (γ), sphere radius (B), asperity tip radius (R), asperity density (η_0), and r.m.s. roughness (σ) for the rough flat need to be supplied. In the current scenario material properties corresponding to AISI 1095 carbon steel is considered. So, the values of elastic modulus, hardness and Poisson's ratio are as follows: E = 200 GPa, H = 6.08 GPa, υ = 0.29. The radius of the sphere (B) is taken as 3 mm. For considering the effect of variation in work of adhesion (γ) on loading behaviour, the following values of surface properties are used: σ = 0.2 μm, R = 250 μm, η_0 = 800 mm−2, z_0 = 0.3 nm. Apart from these parameters three different values of work of adhesion, γ = 5100, 3400 and 476 mJ/m2, are taken into account. Using the above values the elastic adhesion index (θ) and Tabor parameter ($\mu = (R\gamma^2 / E^2 z_o^3)^{1/3}$) are determined and furnished in Table 1.

Elastic adhesion index indicates the relative importance of surface force induced adhesion for elastically deformed asperities when compared with the elastic force on an individual asperity. Table 1. shows that Tabor Parameter is greater than 5 for all the cases, which ensures that JKR regime of adhesion is applicable. These parameters also satisfy the dimensionless Archard's parameter ($\sigma R \eta_0$) of 0.04. In all these cases, the plasticity index ψ comes out as 0.5079. As ψ < 0.6, it indicates that the contact conditions are predominantly elastic in nature. For different combinations of these parameters, the external load (P) is also supplied to evaluate the non-dimensional pressure expressions. For each external applied load, the compliance (α) is calculated from equation (2). This model has a limitation at zero loads as the assumed pressure distribution given by equations (8) and (9) becomes zero. So a small value close to zero is considered in the simulation of zero load situations.

Table 1. Values of elastic adhesion index (θ) and Tabor parameter (μ) corresponding to different work of adhesion (γ)

γ (mJ/m^2)	θ	μ
476	1730	5.60
3400	242.20	20.78
5100	161.46	27.23

The variation of pressure distribution for varying work of adhesion can be seen from Figures 3(a) and 3(b). These figures show the plots of normalized pressure distribution along the contact radius for three different values of work of adhesion at two different loads. It is seen from Figure 3(a) that for low external load (P = 0.001 N) there exists a region of negative pressure (tensile) at the edge of contact. In JKR model, in case of contact between smooth spheres, there always exists a tensile stress singularity at the edge of contact owing to the presence of a surface tension. Therefore, the results obtained here are in agreement with the JKR model. Moreover, the singularity at the edge of contact, which is present in the JKR model, has been replaced by a continuous distribution owing to the effect of roughness. This negative pressure region may be caused by the stretching of the asperities at the edge of contact because of the adhesion effect. However the negative zone is not observed for high load value in Figure 3(b). These figures also show that with an increase in adhesion, the maximum pressure at r = 0 decreases and this can be attributed to the fact that with higher adhesion, the overall contact area increases and this brings down the maximum pressure.

Figures 4(a) and 4(b) show the variation of contact radius and compliance with applied load for varying work of adhesion in the positive range of applied loads. Similar plots of contact radius and compliance with applied load corresponding to different work of adhesion at low and negative load range are presented in Figures 5(a) and 5(b).

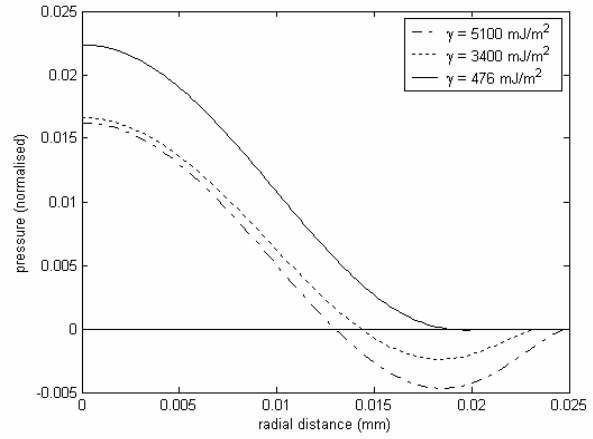

(a)

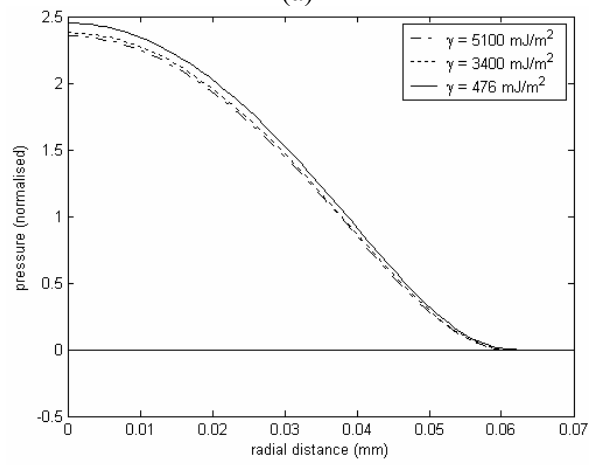

(b)

Figure 3. Pressure distribution for varying work of adhesion (γ = 5100, 3400 and 476 mJ/m^2) at (a) P = 0.001 N and (b) P = 1 N

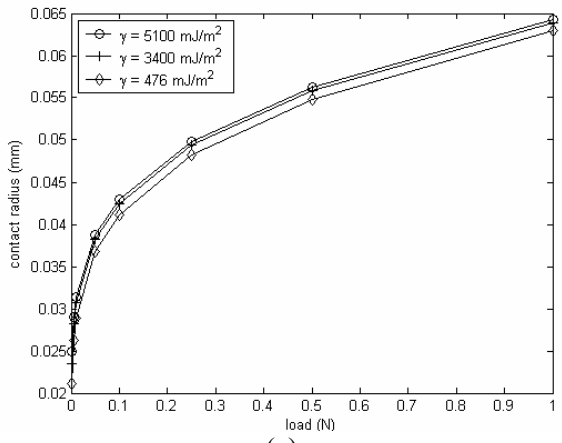

(a)

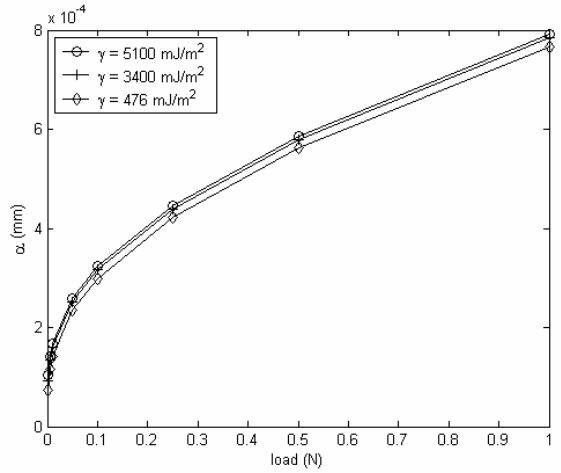

(b)

Figure 4. Variation of (a) contact radius (mm) and (b) compliance (α , mm) with applied load (N) for varying work of adhesion (γ = 5100, 3400 and 476 mJ/m^2)

From Figure 5(a), it is evident that at near zero loads, a finite contact radius exists and high values of γ imply higher contact radius. The negative loading signifies the tensile load required maintaining a particular contact radius, and from this, an idea of the pull on load may be acquired. Figure 5(a) provides a good idea about the pull on loads for varying work of adhesion. It is found that as the adhesive effect increases, the pull-on load also increases. From Figures 4(b) and 5(b), it is clear that for a certain applied load, the value of compliance in high adhesion is more than that in low adhesion. This is easily explained by the fact that with high adhesion, the sphere is pulled more towards the rough flat and hence the compliance is high. In addition, it is seen from these figures that at the initial stages when the applied load is low, the increase in the compliance values is more than that at higher loads.

Figures 6(a) and 6(b) demonstrate the effect of change in sphere radius (B) on variation of compliance and contact radius with applied load. The results are generated for a work of adhesion 5100 mJ/m^2 corresponding to three different value*s* of sphere radius: B = 1, 3, and 6 mm. It is seen that as the sphere radius increases, compliance at a certain load decreases. In fact, throughout the entire load range, the lower sphere radius corresponds to higher compliance. For a certain load, variation in the sphere radius means variation in the contact radius between the sphere and the rough flat. A smaller sphere radius produces a smaller radius of contact and smaller area of contact. As a result, smaller sphere radius leads to higher compliance having higher depth of penetration. Figure 6(b), which shows the variation of contact radius with applied load for different values of sphere radius, lends support to this argument. Figure 7 shows the corresponding pressure distribution at a fixed load for three different sphere radii.

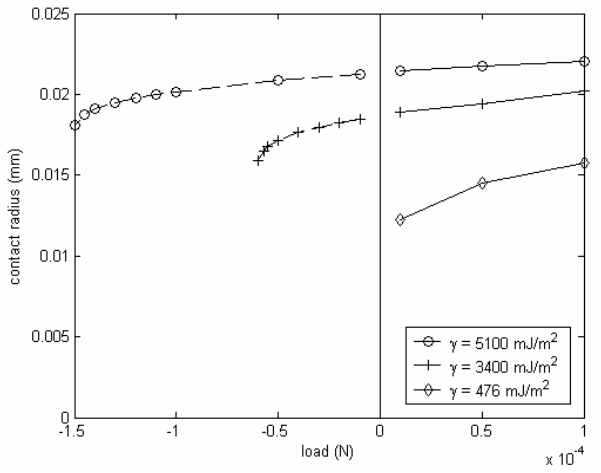

(a)

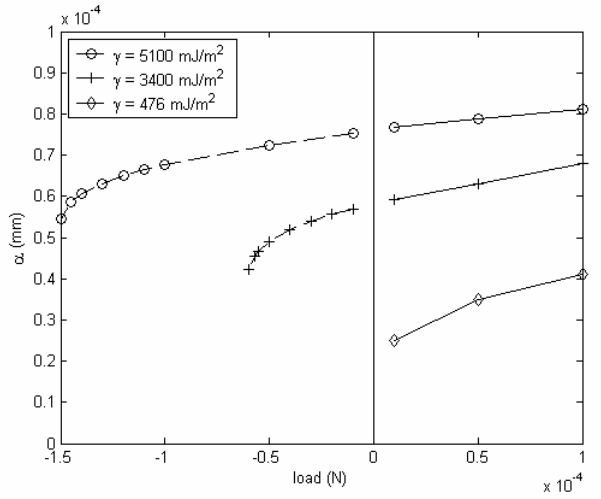

(b)

Figure 5. Variation of (a) contact radius (mm) and (b) compliance (α, mm) with applied load (N) for varying work of adhesion (γ = 5100, 3400 and 476 mJ/m^2) at low and negative load range

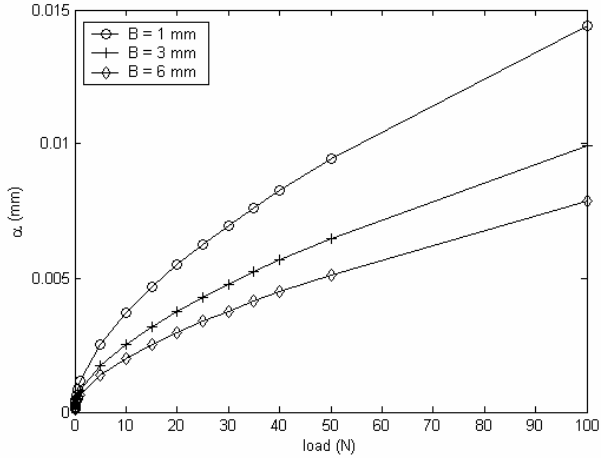

(a)

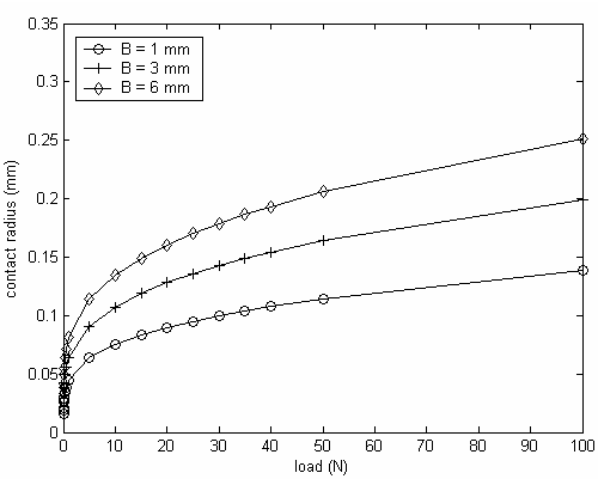

(b)

Figure 6. Variation of (a) compliance (α, mm) and (b) contact radius (mm) with applied load (N) for varying sphere radii

It may be noted here that the present results are applicable for Tabor parameter (μ) greater than 5 implying that the contact is in JKR regime of adhesion. For other ranges of Tabor parameter (μ), the present formulation will not be applicable. One needs to use suitable adhesion models depending on the range of Tabor parameter. For μ<0.1, DMT model [2] needs to be used and for 0.1< μ <5, Maugis model [16] is to be used. Moreover, the material and surface properties considered in present simulations yield the values of plasticity index ψ<0.6 indicating that the contact conditions are predominantly elastic in nature. However, the present model is applicable for all ranges of ψ so long as the adhesion regime is in JKR domain.

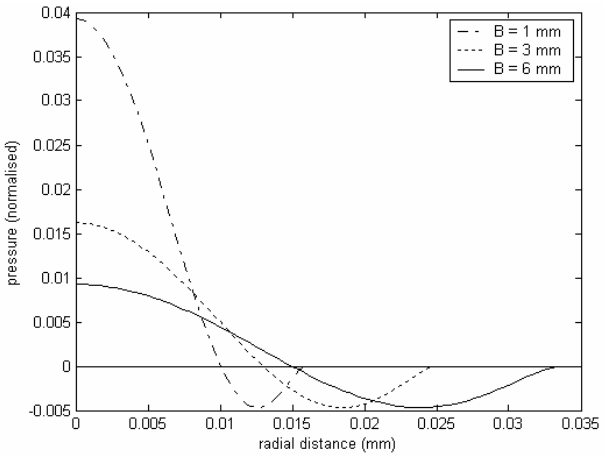

Figure 7. Pressure distribution for varying sphere radii at P = 0.001 N

5. CONCLUSION

The present work considers the contact behaviour of a smooth sphere against a rough flat surface in adhesive contact using a mixed asperity contact model and JKR contacts. The pressure distribution along the radius of contact spot is obtained in terms of well-established elastic adhesion index and plasticity index. The results show a negative pressure region at the edge of contact that may be attributed to the stretching of the asperities because of the adhesion effect in the fringes of contact. This trend is in agreement with the JKR model. The results show that with an increase in adhesion, contact area increases and the maximum compressive pressure comes down. It is observed that larger sphere radius gives lower pressure distribution and lower compliance.

REFERENCES

[1] K.L. Johnson, K. Kendall, A.D. Roberts, *Surface energy and the contact of elastic solids,* Proceedings of the Royal Society A, Vol. 324, pp. 301–313, 1971.

[2] B.V. Derjaguin, V.M. Muller, Y.P. Toporov, *Effect of contact deformation on adhesion of elastic solids,* Journal of Colloid and Interface Science, Vol. 53, pp. 314-326, 1975.

[3] D.Tabor, *Surface forces and surface interactions,* Journal of Colloid and Interface Science, Vol. 58, pp. 2-13, 1977.

[4] V.M. Muller, V.S. Yushchenko, B.V. Derjaguin, *On the influence of molecular forces on the deformation of an elastic sphere and its sticking to a rigid plane,* Journal of Colloid and Interface Science, Vol. 77, pp. 91-101, 1980.

[5] S.K.Roy Chowdhury, P. Ghosh, *Adhesion and adhesional friction at the contact between solids*, Wear, Vol. 174, pp. 9-19, 1994.

[6] J.A. Greenwood, J.B.P. Williamson, *Contact of nominally flat surfaces*, Proceedings of Royal Society A, Vol. 295, pp. 300–319, 1966.

[7] J.A. Greenwood, J.H. Tripp, *The elastic contact of rough spheres,* Journal of Applied Mechanics, Vol. 34, pp. 153–159, 1967.

[8] F.C. Yip, J.E.S. Vernart, *An elastic analysis of the deformation of rough spheres, rough cylinders and rough annuli in contact,* Applied Physics, Vol. 4, pp. 1470-1486, 1971.

[9] K.A. Nuri, *The normal approach between curved surfaces in contact,* Wear, Vol. 30, pp. 321-335, 1974.

[10] B.B. Mikic, R.T. Roca, *A solution to the contact of two rough spherical surfaces,* Journal of Applied Mechanics, Vol. 96, pp. 801–803, 1974.

[11] J. Kagami, K. Yamada, T. Hatazawa, *Contact between a sphere and rough plates,* Wear, Vol. 87, pp. 93–105, 1983.

[12] M. Bahrami, M.M. Yovanovich, J.R. Culham, *A compact model for spherical rough contacts,* Journal of Tribology, Vol. 127, pp. 884-889, 2005.

[13] P. Sahoo, A. Mitra, K. Saha, *Adhesive contact of curved surfaces*, Journal of Engineering Tribology, Vol. 224, pp. 439-451, 2010.

[14] S. K. Roy Chowdhury, H.M. Pollock, *Adhesion between metal surfaces: The effect of surface roughness,* Wear, Vol. 66, pp. 307-321, 1981.

[15] S.P. Timoshenko, J.N. Goodier, *Theory of Elasticity*, 3rd edition, McGraw-Hill, New York, 1970.

[16] D. Maugis, *Adhesion of spheres: the JKR-DMT transition using a Dugdale mode*l, Journal of Colloid and Interface Science, Vol. 150, pp. 243-269, 1992.